Bioconjugate Chemistry

Article

pubs.acs.org/bc

An In-Cell Fluorogenic Tag−Probe System for Protein Dynamics Imaging Enabled by Cell-Penetrating Peptides

Wataru Nomura, Nami Ohashi, Atsumi Mori, and Hirokazu Tamamura*

Institute of Biomaterials and Bioengineering, Tokyo Medical and Dental University 2-3-10 Kandasurugadai, Chiyoda-ku, Tokyo 101-0062, Japan

Supporting Information

ABSTRACT: Fluorogenic probes are useful as molecular tools in chemical biology because they can overcome noise associated with background emission. Previously, using a leucine zipper assembly, we developed a fluorogenically active ZIP tag−probe pair. A probe peptide was designed as an α-helical peptide containing 4-nitrobenzo-2-oxa-1,3-diazole, a solvatochromic fluorescent dye. Tag peptides were designed as antiparallel 2 α-helical peptides, and the tag and probe together form the 3 α-helical bundle structure of the leucine zipper. The use of the system was limited to membrane proteins or targets on the cellular surface because the probe peptide was not compatible with cell penetration. In this study, a challenge for the fluorescent imaging of proteins inside the cells was conducted by development of the ZIP tag−probe system as the second generation. To enable the cell penetration of the probe peptide, the addition of a cell penetrating peptide sequence was tested and a probe peptide with a C-terminal octa-arginine was shown to have high affinity for the tag peptide. In addition to attachment of a CPP structure, pretreatment of cells by 1-pyrenebutyrate enhanced distribution of the probe peptide into the cytosol. Observed colocalization of fluorescence of monomer Kusabira Orange and 4-nitrobenzo-2-oxa-1,3-diazole indicates our fluorogenic tag−probe system can be utilized with tagged proteins. Following stimulation by phorbol ester, the translocation of protein kinase C was tracked by the fluorescence of 4-nitrobenzo-2-oxa-1,3-diazole, suggesting the formation of the noncovalently assembled tag−probe pairing is maintained during the translocation, even when the concentration of the probe peptide is reduced to 0.1 μM. The results indicated that the dynamic change of the protein localization by chemical stimulations can be revealed by the ZIP tag−probe system. Above all, the system is simple to handle and highly compatible with virtually any protein inside the cells.

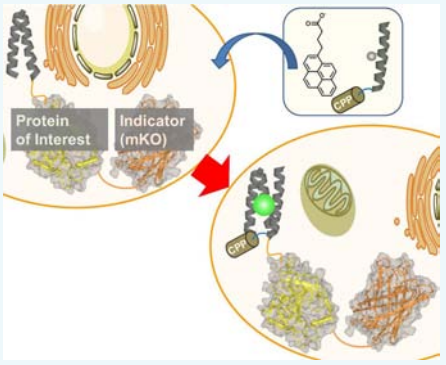

INTRODUCTION

Fluorescent probes are valuable molecular tools in chemical biology and various fluorescent probes to detect small biological components have been developed and used for fluorescent imaging in cells.[1,2] Ratiometric fluorescent probes and fluorogenic probes are particularly useful because they can effectively suppress noise associated with background emission.[3−6] Recently, tag−probe pairs have been developed for the fluorescent imaging of proteins,[7−13] but the number of fluorogenically active tag−probe pairs is still limited.

Green fluorescent protein (GFP) and its homologues are widely used as biological tools for the imaging of protein dynamics in live cells.[14−16] Their fluorescence is well controlled because the fluorophore is located in a unique microenvironment inside a β-barrel structure. On the basis of the unique characteristics of GFP, we previously developed a new tag−probe pair with fluorogenic activity using the leucine zipper assembly, the ZIP tag−probe.[17−19] The tag peptide was designed as two antiparallel α-helical peptides, and the probe was designed as an α-helical peptide, into which a solvatochromic fluorescent dye was incorporated. The environment of the 4-nitrobenzo-2-oxa-1,3-diazole (NBD) attached to the probe peptide changes dramatically from hydrophilic to hydrophobic as a result of the formation of a 3α-helix leucine zipper structure between the tag and the probe peptides, and the bright green fluorescence of the NBD dye is induced in this way. In the first application of fluorescent imaging of proteins, the tag sequence was fused to the N-terminus of the chemokine receptor CXCR4, which is a G protein-coupled receptor (GPCR) correlated with HIV-1 infection, rheumatoid arthritis, and chemotaxis of cancer cells. The imaging of the tag−receptor expressed on the cell surface was successful.[17] If such tag−probe pairs can be utilized intracellularly, the system promises to be a valuable tool for study of protein dynamics because of the rapid increase in fluorescence upon assembly of tag−probe pairs. The previous study showed that the use of the system was limited to membrane proteins or targets on the cellular surface because the probe peptide penetrated cells poorly. Therefore, a second-generation cell-penetrating ZIP tag−probe system was required to resolve this issue and development of the system is reported in this study.

Received: March 15, 2015
Revised: May 2, 2015
Published: May 4, 2015

DOI: 10.1021/acs.bioconjchem.5b00131
Bioconjugate Chem. 2015, 26, 1080−1085

RESULTS AND DISCUSSION

Polyarginine peptides were utilized to increase the cell membrane permeability to the probe peptide. Futaki et al. and Wender et al. have developed the use of polyarginine peptides for transportation of macrobiomolecules to cytoplasm.[20−26] An octa-arginine sequence (R8) was determined as a cell-penetrating peptide (CPP) in the reports. Efficient delivery to the cytoplasm was expected following attachment of this CPP to the probe peptides, and in the first approach, three probe peptides with polyarginine sequences were synthesized (Figure 1). A probe α-helical peptide has an NBD moiety

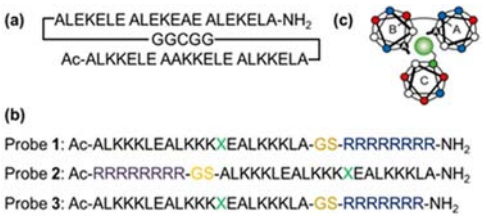

Figure 1. Structures and amino acid sequences of ZIP tag−probe pairs with R8. (a) Sequence of the tag peptide. (b) Sequence of probes **1**−**3**. X = Dap(NBD) (c) A helical wheel model for ZIP tag−probe pairs. Wheels A and B represent the tag peptide, and wheel C represent the probe peptide. Red and blue circles indicate lysine and glutamic acid, respectively.

attached to the side chain of L-α-2,3-diaminopropionic acid (Dap), and the resulting Dap(NBD) residue is situated at a given position in the probe peptide in order to locate the NBD dye in the hydrophobic region of the 3α-helical leucine zipper structure.

In a fluorescent titration with the tag peptide, the fluorescence spectra of the NBD−probe peptides with polyarginines showed a 13−17-fold increase of intensity as the concentration of the tag peptide is increased (Table 1, Supporting Information Figure S1). The emission maximum of the NBD dye shifted from 535 to 505 nm as the emission intensity increased. The three probes showed a reasonable increase of fluorescent intensity, indicating the formation of 3α helical bundles with the tag peptide as the original polyarginine-free probe.[17] The dissociation constants of the probes were markedly different. The apparent dissociation constants (K_d) of the probe peptides **1**−**3** with hepta- or octa-arginine peptides were determined as 181, 894, and 27 nM, respectively, by a nonlinear least-squares curve fitting method based on a 1:1 stoichiometry model[27] (Table 1, Supporting Information Figure S2). Probe **3** with hepta-arginine (R7) showed a strong affinity for the tag peptide. The value was slightly decreased compared to that of the parental probe polyarginine-free peptide.[17] Probe **1** with R8 showed 7-fold decrease in binding affinity compared to that of the probe **3**. The decrease could be rationalized as a consequence of the cationic charges of the polyarginine sequence. The probe peptide was originally cationic because of the rich presence of lysine residues. The addition of the R8 sequence will lead to an increase of +8 in the net charge of the peptide. Probe **2** showed a further 5-fold decrease in binding affinity compared to that of probe **1**. In the assembly of the tag−probe pair, the N-terminus of the probe is located at the side of the loop structure of the tag peptide according to our previous study which utilized the cross-link type probes.[18] Probe **2** has the R8 sequence at the N-terminus of the peptide, and structural conflict between the R8 sequence and the loop structure of the tag peptide should be expected.

Table 1. Emission Maxima, $\Delta I_{max}/I_0$ Values (in Parentheses) of the Probe Peptides and Tag−Probe Complexes, and the Dissociation Constants (K_d) between the Tag and the Probe Peptides

	probe **1**	probe **2**	probe **3**
λ_{max} ($\Delta I_{max}/I_0$)	505 nm (17)	505 nm (13)	506 nm (15)
K_d (nM)[a]	181[b]	894[b]	27[c]

[a]Measurement conditions: 50 mM HEPES buffer solution (pH 7.2, 100 mM NaCl), at 25 °C, [probe] = 0.5 μM. [b]Determined by the fluorescent intensity change at 505 nm. [c]Determined by the fluorescent intensity change at 506 nm.

The function of R8 peptide as a CPP has been intensively studied as reported previously.[28−30] Several researchers have shown however that R8 residues are not absolutely required for cell penetration of more complex peptides.[31] Thus, we have addressed the cell permeability of probes **1** and **3** at 5 μM by utilizing fluorescein-labeled probes **4** and **5** (Supporting Information Figure S3). The probes were added to HeLa cells, and after incubation for 30 min at 37 °C under an atmosphere containing 5% CO_2, the cells were washed with PBS and mounted on a confocal laser scanning microscope. Both of the probes showed similar efficiency in cell permeability and cytotoxicity (Supporting Information Figure S4). As a consequence, we concluded that probe **1** is appropriate to the further study of cell permeability at lower concentrations and protein imaging within the cytosol as it shows reasonable binding affinity for the tag peptide and a greater increase in fluorescent intensity than probe **3**.

Before studying formation of tag−probe pairing within cells, the tag−probe pairing properties of probe **1** were assessed with circular dichroism (CD) spectra (Figure 2). In the CD study,

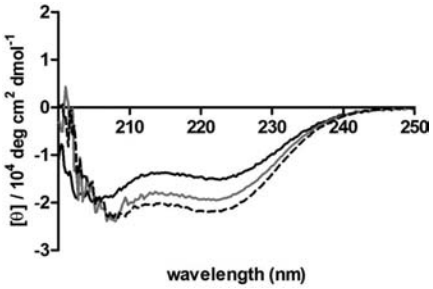

Figure 2. CD spectra of probe **1** (black line), tag peptide (gray line), and tag−probe **1** complex (dashed line).

probe **1** and the tag peptides showed patterns in the CD spectra typical of α-helical structures with double minima at 208 and 222 nm. When the two peptides are mixed in an equimolar ratio, the spectra showed the deepest minima and the α-helical contents of probe **1**, tag, and the mixture of tag and probe **1** were determined by a standard method[32] to be 43.5%, 53.2%, and 57.5%, respectively. Compared to each individual peptide, the α helical content of tag−probe pairing is increased indicating that each helix is stabilized by formation of a 3α helix bundle in a tag−probe assembly.

The membrane permeability of probe **1** at 1 μM was further addressed (Supporting Information Figure S5). Under this condition, the fluorescence from the probes was not distributed

DOI: 10.1021/acs.bioconjchem.5b00131
Bioconjugate Chem. 2015, 26, 1080−1085

throughout the cytosol, but rather, formation of vesicles in the cytosol and aggregation on the outer membrane with bright fluorescence was observed even in the absence of the target tag-peptide. Thus, a method to deliver R8 peptides efficiently to the cytosol was adopted by utilizing 1-pyrenebutyrate as its counteranion.[33,34] Detailed studies have been reported concerning functions and mechanisms of this method in model systems based on liposomes,[28−30] and it has been suggested that the counteranion-mediated phase transfer mechanism can be applied to the translocation of R8 peptides across lipid bilayer of cells. The effect of 1-pyrenebutyrate provides successful distribution of R8 peptides to the cytosol in contrast to endocytosis-mediated cellular incorporation, in which the peptides will be capsulated in the endosomes. As a target protein, a gene of mKO-tag fusion protein was introduced to the mammalian expression vector and the plasmid DNA coding the fusion protein was transiently transfected to HeLa cells by electropermeabilization (Neon, Life technologies). After transfection for 48 h, experiments for cell penetration and pairing formation with the tag peptide region were performed. The fluorescence from mKO showed that mKO-tag fusion protein was distributed between the cytosol and the nuclei in cells. This observation suggests that the mKO fluorescent protein does not show any specific localization in the cells when it contains only the tag peptide sequence and the fluorescence from NBD merged with mKO fluorescence. This result indicates that probe **1** was successfully distributed to whole cells and that the tag−probe pair was formed with the mKO-tag fusion protein (Figure 3a).

With the successful observation of tag−probe formation between probe **1** and mKO-tag fusion protein, which lacks specific localization in the cells, we performed the detection of tagged-proteins that are localized in specific organelles in mammalian cells. Two fusion proteins were prepared, one with ER-retention signal peptides from calreticulin and one with histone protein, H2B. These proteins were expressed in the same manner, and cells were treated with 1-pyrenebutyrate and 0.1 μM concentration of probe **1**. As anticipated, each protein was found to be localized in the cells, in cytosol for ER-mKO-tag and in nuclei for H2B-mKO-tag as shown in the left panels of Figures 3b,c, respectively. The result showed that probe **1** could be utilized for detection of specifically localized proteins in the cytosol (Figure 3b) and in the nuclei (Figure 3c). The protein with the ER retention signal peptide will be expressed in the compartment structure. It is of interest that the protein in the organelle compartment can be detected by the tag−probe pair system, and this result suggests that treatment with 1-pyrenebutyrate allow the R8-peptide to render the membrane structure in the cytosol permeable.

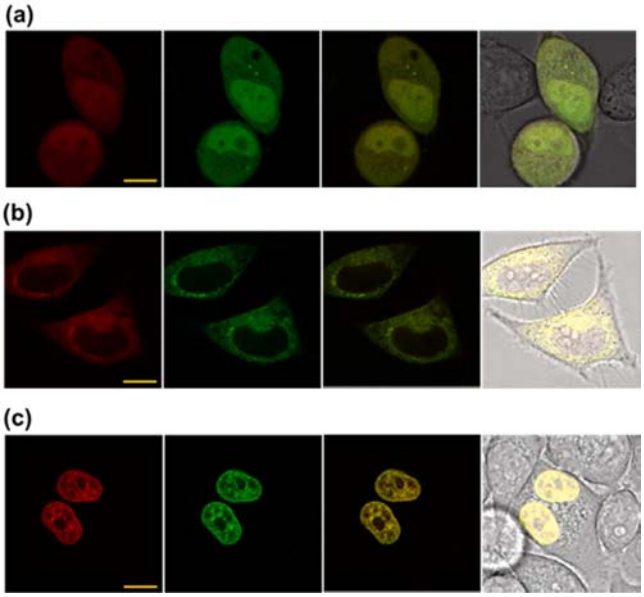

Figure 3. Fluorescent imaging by fluorogenic probe **1**. HeLa cells were pretreated with 1-pyrenebutyrate. Panels in (a−c) show the mKO signal, the NBD signal, the merge of NBD and mKO signals, and the merged image with the differential interference contrast (DIC) image (from left to right). Tagged-mKO fusion proteins are (a) mKO-tag only, (b) ER-mKO-tag with the ER retention signal peptide, and (c) H2B-mKO-tag. For excitation, beam splitter 488/552 was employed. Multiband channels 495−545 and 562−630 (nm) were utilized for imaging of emission from NBD and mKO, respectively. The scale bars indicate 10 μm.

It would be useful if the protein imaging technique could enable the visualization of protein dynamics with noncovalently attached probes. Accordingly, we observed the dynamic change of localization by addition of different chemicals. Protein kinase C (PKC) isoforms play pivotal roles in physiological responses to growth factors and oxidative stress mediated through the endogenous second messenger 1,2-diacylglycerol (DAG). Such responses regulate numerous cellular processes,[35,36] including proliferation,[37] differentiation,[38] migration,[39] and apoptosis,[40,41] and the tumor promoting phorbol esters, potent surrogates of DAG, provide a convenient probe of the PKC function. Ligand binding to the C1b domain of PKC leads to membrane translocation. This translocation of PKC is of central importance for its function because the localization of PKC determines the substrates it accesses.[42] As a ligand inducing membrane translocation of PKC, phorbol 12,13-dibutyrate (PDBu) was utilized.

In the absence of PDBu, expressed PKCδ-mKO-tag fusion was distributed in the cytosol and the NBD fluorescence indicated that PKCδ and probe **1** at a concentration of 0.1 μM formed a tag−probe pair and were consequently colocalized (Figure 4a). When the probe concentration was increased to 1 μM, nonspecific fluorescence from NBD channel at the cell membrane was observed, suggesting that the probe concentration is optimum at 0.1 μM (Supporting Information Figure S6). One minute after the addition of 10 μM of PDBu, the fluorescence from mKO revealed translocation of PKCδ (Figure 4b). The translocation was more progressed at 10 min after the addition of PDBu (Figure 4c). It is reported that PKCδ interacts with mitochondria by a novel and isozyme-specific mechanism distinct from its canonical recruitment to other membranes such as the plasma membrane or Golgi following stimulation with phorbol esters.[43−45] Most of the fluorescence from NBD showed cotranslocation as with PKCδ (Figures 4b−d). In comparison of fluorescent intensity along the cross section shown in Figure 4e, fluorescence in the nuclei is decreased and it is increased around the nuclear membrane after addition of PDBu. In addition, accumulation of fluorescence is observed in the cytosol. These results suggest that the tag−probe complex is very stable and not disrupted by a dynamic change in the localization of target proteins.

■ CONCLUSIONS

Experiments with the second-generation cell-penetrating ZIP tag−probe system showed that the dynamic change of the

DOI: 10.1021/acs.bioconjchem.5b00131
Bioconjugate Chem. 2015, 26, 1080−1085

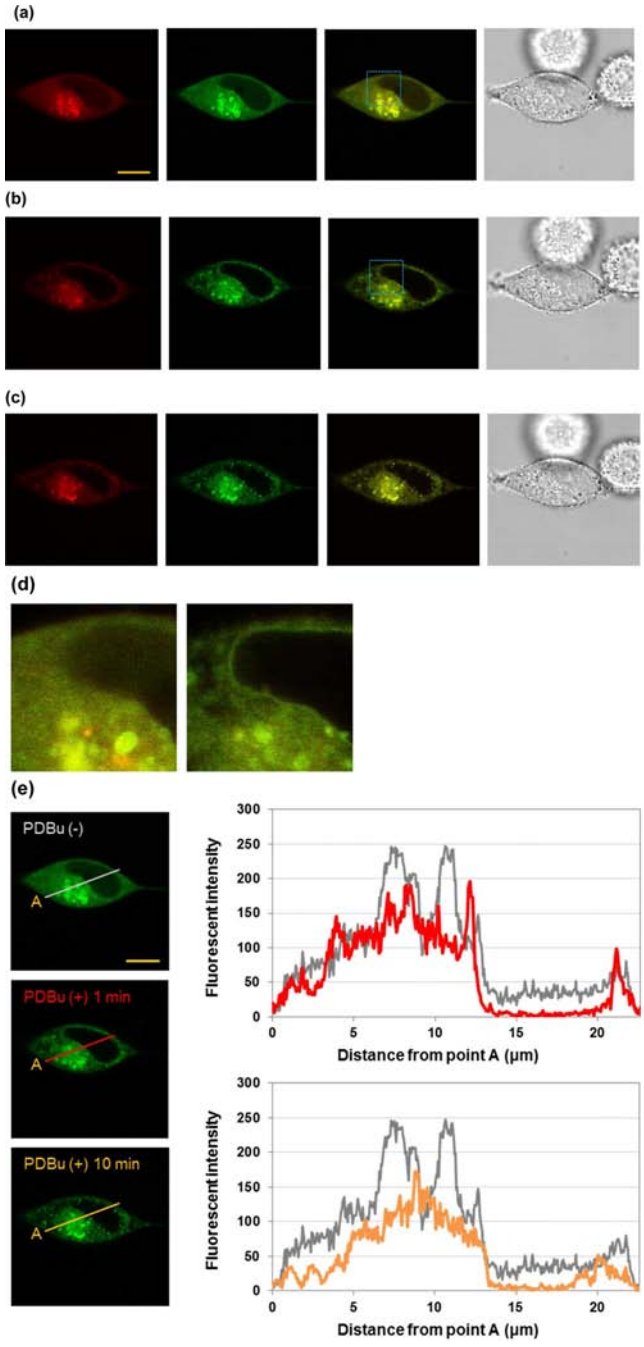

Figure 4. Fluorescent imaging of ligand-induced PKCδ-mKO-tag translocation by probe **1**. HeLa cells were pretreated with 1-pyrenebutyrate. (a) Before the addition of PDBu, probe **1** at 0.1 μM is colocalized with PKC in the cytosol. (b,c) As translocation of PKCδ-mKO-tag was induced by the addition of 10 μM PDBu, the NBD signal was colocalized with the signal from PKCδ-mKO-tag fusion protein. The fluorescent images in (b) and (c) are those of 1 and 10 min after addition of PDBu, respectively. Panels in (a–c) shows the mKO signal, the NBD signal, the merge of NBD and mKO signals, and the differential interference contrast (DIC) image (from left to right). (d) Magnified images of the area of interest to show the detailed translocation of PKCδ by addition of PDBu. The left and right panels are from the boxed area in merged image of NBD and mKO of panels (a) and (b), respectively. (e) Comparison of fluorescent intensity changed after the addition of 10 μM PDBu. The upper and lower graphs show changes at 1 and 10 min, respectively. The gray, red, and orange lines in the graphs indicate the fluorescent intensity along the lines in the panels showing before, 1 and 10 min after the addition of PDBu, respectively. For excitation, beam splitter 488/552 was employed. Multiband channels 495–545 (nm) and 562–630 (nm) were utilized for imaging emission from NBD and mKO, respectively. The scale bars indicate 10 μm.

protein localization inside the cells by chemical stimulations can be visualized. Preparations of a protein of interest with the tag peptide and procedures for fluorescent imaging are simple and accessible, and the required concentration of the probe peptide can be as low as 0.1 μM. The formation of noncovalently assembled tag–probe complexes has been shown to be tolerant to change of pH in vitro in a range of physiological conditions. The protein of interest could be any protein because the tag–probe formation is independent of the protein structure. Intracellular fluorescent imaging of target molecules depends largely on the cell permeability of probe molecules.[46] Our strategy could enhance the options of molecular imaging inside the cells because the turn-on fluorescent system can increase the signal/noise ratio and the cell permeability is controlled by probe peptides. Because previously reported that standard peptide synthesis is used, diverse fluorescent dyes such as 7-diethylaminocoumarin-3-carboxylic acid (DEAC) can be adopted.[19] To expand the range of fluorescent colors, other fluorescent techniques such as Foster resonance of energy transfer (FRET) could be applied. In addition, the multicolor imaging during pulse-chase observation can also be achieved by our DEAC tag–probe system inside the cells, the applications of which were limited previously to in vitro experiments.[19] Time-lapse imaging of protein expression/translocation for a longer time period may be desirable, but it is not clear how stable the tag–probe complex in a noncovalent assembly manner is inside the cells. The use of cross-link-type tag–probe pairs[18] for fluorescent imaging inside the cells is the subject of future studies.

EXPERIMENTAL PROCEDURES

General Methods. For analytical HPLC, a Cosmosil $_5C_{18}$-ARII column (4.6 mm × 250 mm, Nacalai Tesque, Inc., Kyoto, Japan) was employed with a linear gradient of CH_3CN containing 0.1% (v/v) TFA at a flow rate of 1 cm^3 min^{-1} on a LaChrom Elite HTA system (Hitachi High-Technologies Corporation, Ltd., Tokyo, Japan). Eluted products were detected by UV-absorption at 220 nm. Preparative HPLC was performed using a Cosmosil $_5C_{18}$-ARII column (20 mm × 250 mm, Nacalai Tesque, Inc.) on a JASCO PU-2089 plus (JASCO Corporation, Ltd., Tokyo, Japan) in a suitable gradient mode of CH_3CN solution containing 0.1% (v/v) TFA at a flow rate of 7 cm^3min^{-1}. Eluted products were detected by UV absorption at 220 nm. UV spectra were recorded using a JASCO V650 UV–vis spectrophotometer.

Synthesis of Tag and Probe Peptides. The tag peptide was prepared as described previously.[17] Details of probe syntheses are provided in the Supporting Information.

Fluorescence Titration Analysis. Fluorescence spectra were recorded with JASCO FP-6600 using a quartz cell. A stock solution of the probe peptide was diluted with 50 mM HEPES buffer solution (pH 7.2, 100 mM NaCl) to prepare a solution with a final concentration (0.5 μM). The corresponding tag peptide solution was added dropwise to a 0.5 μM probe peptide solution, and the fluorescence spectra (λex =456 nm) were measured at 25 °C. An average value of three measurements

DOI: 10.1021/acs.bioconjchem.5b00131
Bioconjugate Chem. 2015, 26, 1080–1085

was plotted as each point. Fluorescent titration curves (λ_{em} = 505 nm for probes **1** and **2**, and 506 nm for probe **3**) were analyzed with a nonlinear least-squares curve-fitting method utilizing GraphPad Prism 5 to evaluate K_d values.

Construction of Expression Plasmids, Mammalian Cell Culture, Transfection, and Fluorescent Imaging. Detailed methods of the construction of plasmid encoding mKO-fusion proteins are described in Supporting Information. HeLa cells were maintained in DMEM complete medium (10% FBS/penicillin/strepemycin). For electropermeabilization, 5×10^5 cells were collected. Then 2 μg per tube of each plasmid DNA encoding an mKO fusion protein, mKO-tag, ER-mKO-tag, H2B-mKO-tag, or PKCδ-mKO-tag was added. The nucleofection was performed in 100 μL of solution by following the instruction provided by the manufacturer. Cells were divided into two 35 mm glass-bottom dishes and cultured for 48 h. For fluorescent imaging, a TSC SP8 (Leica) confocal laser-scanning microscope equipped with a 40× objective lens was utilized.

Treatment Cells with 1-Pyrenebutyrate. 1-Pyrenebutyrate was prepared as a 1 mM stock solution in DMSO. The stock solution was diluted to 1.1 μM by Hanks' Balanced Salt Solution (HBSS). Then 450 μL of the 1-pyrenebutyrate solution was added to cells seeded in glass-bottom dishes. After incubation for 2 min at rt, 50 μL of the 1 μM probe solution was added and incubated for 4 min under 5% CO_2 at 37 °C, and without washing, the dishes were mounted on a TSC SP8 (Leica) confocal laser-scanning microscope equipped with a 40× objective lens.

Tracking PKC-Translocation Induced by Addition of PDBu. PKCδ-mKO-tag fusion protein was expressed in HeLa cells as described above. After 48 h, the cells were treated with 1 μM of 1-pyrenebutyrate and 0.1 μM of probe **1**. The pretranslocation image was taken immediately after this treatment by the TSC SP8 (Leica) confocal laser-scanning microscope equipped with a 40× objective lens. For addition of PDBu, 10 mM stock solution was added directly to glass bottom dishes at a final concentration at 10 μM. Then 1 and 10 min after the PDBu addition, the translocation of PKCδ-mKO-tag fusion protein was observed on the confocal microscope (Supporting Information Figure S7).

■ ASSOCIATED CONTENT

Ⓢ Supporting Information

Detailed experimental procedures, peptide synthesis, HPLC charts, plasmid construction, and control imaging experiments. The Supporting Information is available free of charge on the ACS Publications website at DOI: 10.1021/acs.bioconjchem.5b00131.

■ AUTHOR INFORMATION

Corresponding Author

*E-mail: tamamura.mr@tmd.ac.jp.

Notes

The authors declare no competing financial interest.

■ ACKNOWLEDGMENTS

This work was supported in part by JSPS Core-to-Core Program, A, Advanced Research Networks, the Asahi Glass Foundation (H.T.), and the Platform for Drug Discovery, Informatics, and Structural Life Science of MEXT, Japan.

■ REFERENCES

(1) *Topics in Fluorescence Spectroscopy, Vol. 9, Advanced Concepts in Fluorescence Sensing, Part A: Small Molecule Sensing* (2005) (Geddes, C. D., and Lakowicz, J. R., Eds.) Springer, New York.
(2) *Topics in Fluorescence Spectroscopy, Vol. 9, Advanced Concepts in Fluorescence Sensing, Part B: Macromolecular Sensing* (2005) (Geddes, C. D., and Lakowicz, J. R., Eds.) Springer, New York.
(3) Terai, T., and Nagano, T. (2008) Fluorescent probes for bioimaging applications. *Curr. Opin. Chem. Biol. 12*, 515−521.
(4) Grynkiewicz, G., Poenie, M., and Tsien, R. Y. (1985) A new generation of Ca^{2+} indicators with greatly improved fluorescence properties. *J. Biol. Chem. 260*, 3440−3450.
(5) Ojida, A., Takashima, I., Kohira, T., Nonaka, H., and Hamachi, I. (2008) Turn-on fluorescence sensing of nucleoside polyphosphates using a xanthene-based Zn(II) complex chemosensor. *J. Am. Chem. Soc. 130*, 12095−12101.
(6) Yano, Y., Yano, A., Oishi, S., Sugimoto, Y., Tsujimoto, G., Fujii, N., and Matsuzaki, K. (2008) Coiled-coil tag−probe system for quick labeling of membrane receptors in living cell. *ACS Chem. Biol. 3*, 341−345.
(7) Griffin, B. A., Adams, S. R., and Tsien, R. Y. (1998) Specific covalent labeling of recombinant protein molecules inside live cells. *Science 281*, 269−272.
(8) Guignet, E. G., Hovius, R., and Vogel, H. (2004) Reversible site-selective labeling of membrane proteins in live cells. *Nature Biotechnol. 22*, 440−444.
(9) Ojida, A., Honda, K., Shinmi, D., Kiyonaka, S., Mori, Y., and Hamachi, I. (2006) Oligo-Asp tag/Zn(II) complex probe as a new pair for labeling and fluorescence imaging of proteins. *J. Am. Chem. Soc. 128*, 10452−10459.
(10) Keppler, A., Gendreizig, S., Gronemeyer, T., Pick, H., Vogel, H., and Johnsson, K. (2003) A general method for the covalent labeling of fusion proteins with small molecules in vivo. *Nature Biotechnol. 21*, 86−89.
(11) Stöhr, K., Siegberg, D., Lymperopoulos, K., Öz, S., Schulmeister, S., Pfeifer, A. C., Bachmann, J., Klingmüller, U., Sourjik, V., and Herten, D. P. (2010) Quenched substrates for live-cell labeling of SNAP-tagged fusion proteins with improved fluorescent background. *Anal. Chem. 82*, 8186−8189.
(12) Los, G. V., Darzins, A., Karassina, N., Zimprich, C., Learish, R., McDougall, M. G., Encell, L. P., Friedman-Ohana, R., Wood, M., Vidugiris, G., et al. (2005) How to construct and use a HaloTag coding region control expression vector. *Promega Cell Notes 11*, 2−6.
(13) Mizukami, S., Watanabe, S., Hori, Y., and Kikuchi, K. (2009) Covalent protein labeling based on noncatalytic β-lactamase and a designed FRET substrate. *J. Am. Chem. Soc. 131*, 5016−5017.
(14) Shimomura, O., Johnson, F. H., and Saiga, Y. (1962) Extraction, purification and properties of aequorin, a bioluminescent protein from the luminous hydromedusan, Aequorea. *J. Cell. Comp. Physiol. 59*, 223−239.
(15) Zimmer, M. (2002) Green fluorescent protein (GFP): applications, structure, and related photophysical behavior. *Chem. Rev. 102*, 759−781.
(16) Tsien, R. Y. (2005) Building and breeding molecules to spy on cells and tumors. *FEBS Lett. 579*, 927−932.
(17) Tsutsumi, H., Nomura, W., Abe, S., Mino, T., Masuda, A., Ohashi, N., Tanaka, T., Ohba, K., Yamamoto, N., Akiyoshi, K., and Tamamura, H.. (2009) Fluorogenically active leucine zipper peptides as tag−probe pairs for protein imaging in living cells. *Angew. Chem., Int. Ed. 48*, 9164−9166.
(18) Nomura, W., Mino, T., Narumi, T., Ohashi, N., Masuda, A., Hashimoto, C., Tsutsumi, H., and Tamamura, H. (2010) Development of crosslink-type tag−probe pairs for fluorescent imaging of proteins. *Biopolymers: Pept. Sci. 94*, 843−852.
(19) Tsutsumi, H., Abe, S., Nomura, W., and Tammaura, H. (2011) Intense blue fluorescence in a leucine zipper assembly. *ChemBioChem 12*, 691−694.
(20) Futaki, S., Suzuki, T., Ohashi, W., Yagami, T., Tanaka, S., Ueda, K., and Sugiura, Y. (2001) Arginine-rich peptides. An abundant source

DOI: 10.1021/acs.bioconjchem.5b00131
Bioconjugate Chem. 2015, 26, 1080−1085

of membrane-permeable peptides having potential as carriers for intracellular protein delivery. *J. Biol. Chem. 276*, 5836−5840.
(21) Nakase, I., Niwa, M., Takeuchi, T., Sonomura, K., Kawabata, N., Koike, Y., Takehashi, M., Tanaka, S., Ueda, K., Simpson, J. C., et al. (2004) Cellular uptake of arginine-rich peptides: roles for macropinocytosis and actin rearrangement. *Mol. Ther. 10*, 1011−1022.
(22) Futaki, S. (2005) Membrane-permeable arginine-rich peptides and the translocation mechanisms. *Advanced Drug Delivery Rev. 57*, 547−558.
(23) Kosuge, M., Takeuchi, T., Nakase, I., Jones, A. T., and Futaki, S. (2008) Cellular internalization and distribution of arginine-rich peptides as a function of extracellular peptide concentration, serum, and plasma membrane associated proteoglycans. *Bioconjugate Chem. 19*, 656−664.
(24) Wender, P. A., Mitchell, D. J., Pattabiraman, K., Pelkey, E. T., Steinman, L., and Rothbard, J. B. (2000) The design, synthesis, and evaluation of molecules that enable or enhance cellular uptake: peptoid molecular transporters. *Proc. Natl. Acad. Sci. U. S. A. 97*, 13003−13008.
(25) Rothbard, J. B., Garlington, S., Lin, Q., Kirschberg, T., Kreider, E., McGrane, P. L., Wender, P. A., and Khavari, P. A. (2000) Conjugation of arginine oligomers to cyclosporin A facilitates topical delivery and inhibition of inflammation. *Nature Med. 6*, 1253−1257.
(26) Rothbard, J. B., Jessop, T. C., and Wender, P. A. (2005) Adaptive translocation: the role of hydrogen bonding and membrane potential in the uptake of guanidinium-rich transporters into cells. *Adv. Drug Delivery Rev. 57*, 495−504.
(27) Kuwabara, T., Nakamura, A., Ueno, A., and Toda, F. (1994) Inclusion complexes and guest-induced color changes of pH-indicator-modified β-cyclodextrins. *J. Phys. Chem. 98*, 6297−6303.
(28) Sakai, N., Takeuchi, T., Futaki, S., and Matile, S. (2005) Direct observation of anion-mediated translocation of fluorescent oligoarginine carriers into and across bulk liquid and anionic bilayer membranes. *ChemBioChem 6*, 114−122.
(29) Perret, F., Nishihara, M., Takeuchi, T., Futaki, S., Lazar, A. N., Coleman, A. W., Sakai, N., and Matile, S. (2005) Anionic fullerenes, calixarenes, coronenes, and pyrenes as activators of oligo/polyarginines in model membranes and live cells. *J. Am. Chem. Soc. 127*, 1114−1115.
(30) Nishihara, M., Perret, F., Takeuchi, T., Futaki, S., Lazar, A. N., Coleman, A. W., Sakai, N., and Matile, S. (2005) Arginine magic with new counterions up the sleeve. *Org. Biomol. Chem. 3*, 1659−1669.
(31) B. Smith, B., Daniels, D. S., Coplin, A., Jordan, G., McGregor, L., and Schepartz, A. (2008) Minimally cationic cell-permeable miniature proteins via alpha-helical arginine display. *J. Am. Chem. Soc. 130*, 2948−2949.
(32) Jackson, D. Y., King, D. S., Chmielewski, J., Singh, S., and Schultz, P. G. (1991) General approach to the synthesis of short α-helical peptides. *J. Am. Chem. Soc. 113*, 9391−9392.
(33) Takeuchi, T., Kosuge, M., Tadokoro, A., Sugiura, Y., Nishi, M., Kawata, M., Sakai, N., Matile, S., and Futaki, S. (2006) Direct and rapid cytosolic delivery using cell-penetrating peptides mediated by pyrenebutyrate. *ACS Chem. Biol. 1*, 299−303.
(34) Inomata, K., Ohno, A., Tochio, H., Isogai, S., Tenno, T., Nakase, I., Takeuchi, T., Futaki, S., Ito, Y., Hiroaki, H., and Shirakawa, M. (2009) High-resolution multi-dimensional NMR spectroscopy of proteins in human cells. *Nature 458*, 106−109.
(35) Nishizuka, Y. (1992) Intracellular signaling by hydrolysis of phospholipids and activation of protein kinase C. *Science 258*, 607−614.
(36) Newton, A. C. (1995) Protein kinase C: structure, function, and regulation. *J. Biol. Chem. 270*, 28495−28498.
(37) Watanabe, T., Ono, Y., Taniyama, Y., Hazama, K., Igarashi, K., Ogita, K., Kikkawa, U., and Nishizuka, Y. (1992) Cell division arrest induced by phorbol ester in CHO cells overexpressing protein kinase C-δ subspecies. *Proc. Natl. Acad. Sci. U. S. A. 89*, 10159−10163.
(38) Mischak, H., Pierce, J. H., Goodnight, J., Kazanietz, M. G., Blumberg, P. M., and Mushinski, J. F. (1993) Phorbol ester-induced myeloid differentiation is mediated by protein kinase C-α and -δ and not by protein kinase C-βII, -ε, -ζ, and -η. *J. Biol. Chem. 268*, 20110−20115.
(39) Li, C., Wernig, F., Leitges, M., Hu, Y., and Xu, Q. (2003) Mechanical stress-activated PKCδ regulates smooth muscle cell migration. *FASEB J. 17*, 2106−2108.
(40) Ghayur, T., Hugunin, M., Talanian, R. V., Ratnofsky, S., Quinlan, C., Emoto, Y., Pandey, P., Datta, R., Huang, Y., Kharbanda, S., et al. (1996) Proteolytic activation of Protein Kinase C δ by an ICE/CED 3-like protease induces characteristics of apoptosis. *J. Exp. Med. 184*, 2399−2404.
(41) Alkon, D. L., Sun, M.-K., and Nelson, T. J. (2007) PKC signaling deficits: a mechanistic hypothesis for the origins of Alzheimer's disease. *Trends Pharmacol. Sci. 28*, 51−60.
(42) Wang, Q. J. (2006) PKD at the crossroads of DAG and PKC signaling. *Trends Pharmacol. Sci. 27*, 317−323.
(43) Li, L., Lorenzo, P. S., Bogi, K., Blumberg, P. M., and Yuspa, S. H. (1999) Protein kinase Cdelta targets mitochondria, alters mitochondrial membrane potential, and induces apoptosis in normal and neoplastic keratinocytes when overexpressed by an adenoviral vector. *Mol. Cell. Biol. 19*, 8547−8558.
(44) Majumder, P. K., Pandey, P., Sun, X., Cheng, K., Datta, R., Saxena, S., Kharbanda, S., and Kufe, D. (2000) Mitochondrial translocation of Protein Kinase C δ in phorbol ester-induced cytochrome c release and apoptosis. *J. Biol. Chem. 275*, 21793−21796.
(45) Wu-Zhang, A. X., Murphy, A. N., Bachman, M., and Newton, A. C. (2012) Isozyme-specific interaction of protein kinase Cδ with mitochondria dissected using live cell fluorescence imaging. *J. Biol. Chem. 287*, 37891−37906.
(46) Myochin, T., Hanaoka, K., Komatsu, T., Terai, T., and Nagano, T. (2012) Design strategy for a near-infrared fluorescence probe for matrix metalloproteinase utilizing highly cell permeable boron dipyrromethene. *J. Am. Chem. Soc. 134*, 13730−13737.

DOI: 10.1021/acs.bioconjchem.5b00131
Bioconjugate Chem. 2015, 26, 1080−1085